



Fermi National Accelerator Laboratory

FERMILAB-Conf-92/369

**The DØ Inter-Cryostat Detector,
Massless Gaps and Missing E_T Resolution**

Kathleen Streets
for the DØ Collaboration

*University of Maryland
College Park, Maryland 20742*

*Fermi National Accelerator Laboratory,
P.O. Box 500, Batavia, Illinois 60510*

December 1992

Presented at the *Third International Conference on Calorimetry in High Energy Physics*,
Corpus Christi, Texas, September 29-October 2, 1992



Disclaimer

This report was prepared as an account of work sponsored by an agency of the United States Government. Neither the United States Government nor any agency thereof, nor any of their employees, makes any warranty, express or implied, or assumes any legal liability or responsibility for the accuracy, completeness, or usefulness of any information, apparatus, product, or process disclosed, or represents that its use would not infringe privately owned rights. Reference herein to any specific commercial product, process, or service by trade name, trademark, manufacturer, or otherwise, does not necessarily constitute or imply its endorsement, recommendation, or favoring by the United States Government or any agency thereof. The views and opinions of authors expressed herein do not necessarily state or reflect those of the United States Government or any agency thereof.

THE DØ INTER-CRYOSTAT DETECTOR, MASSLESS GAPS AND MISSING E_T RESOLUTION *

Kathleen Streets
University of Maryland
College Park, MD 20742, USA

THE DØ COLLABORATION

ABSTRACT

The inter-cryostat detector and massless gaps are located in the intermediate rapidity regions between the central and end calorimeters of the DØ detector and are designed to improve energy measurements in those regions. Results are presented from test beam and collider data showing the improvement of single particle and jet energy resolutions with the inclusion of the inter-cryostat detector and massless gaps. The calorimeter missing E_T resolution in collider data is presented.

1. Introduction

The DØ detector features a uranium and liquid argon calorimeter¹ which is divided into three separate cryostats. The central calorimeter (CC) and the two endcap calorimeters (EC) each contain electromagnetic and hadronic modules. The massless gaps and inter-cryostat detectors are located in the intermediate rapidity region, between the central and endcap calorimeters. Figure 1a shows the layout of the central and endcap calorimeters and the boundaries of the intermediate rapidity region.

The improvement of the energy measurement obtained by using the inter-cryostat detectors and massless gaps for single particles and jets is presented in this paper. Further results on the response of the calorimeter to electron, pions and jets can be found elsewhere².

The missing E_T of events as measured by the calorimeter is an important component in the measurement of the W mass and of new particle searches. The resolution of the missing E_T (\cancel{E}_T) from minimum bias collider data is presented in this paper.

2. Design of Inter-Cryostat Detector and Massless Gaps

The inter-cryostat detector (ICD) and massless gaps (MG) were designed³ to improve the energy measurement and resolution in the region between the central and endcap calorimeters of the DØ detector by providing additional sampling of the

*This work was supported in part by the U.S. Department of Energy and the U.S. National Science Foundation.

³Presented at The Third International Conference on Calorimetry in High Energy Physics, Sept 29 - Oct 2, 1992 at Corpus Christi, TX

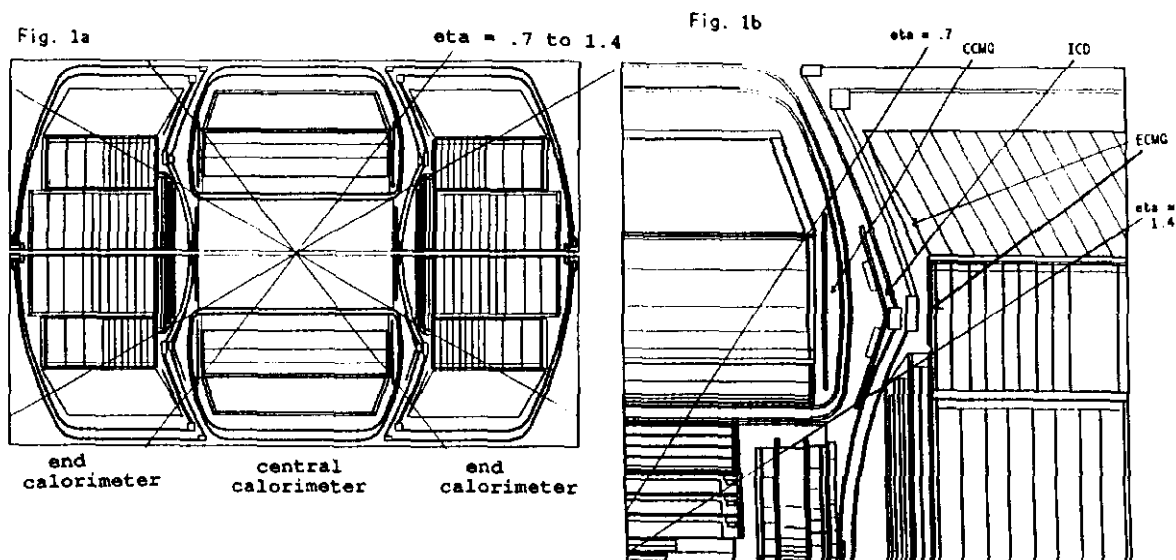


Figure 1: a). side view of DØ calorimeter, b). side view of inter-cryostat region

shower energy. The inter-cryostat region covers the pseudorapidity ($\eta \equiv -\ln \tan\theta/2$) range $0.7 < |\eta| < 1.4$, where θ is the polar angle from the beam axis. In this region, the showers propagate through both the central and end calorimeters. The energy measurements are degraded by the presence of support walls, end plates of the calorimeter modules, and the cryostat walls and lack of uniform liquid-argon calorimetry. Figure 1b shows a detail of the side view of this region.

The inter-cryostat detector modules are made from plastic scintillator tiles with embedded polystyrene wavelength shifting fibers and are read out through 1/2 inch diameter photomultiplier tubes. Each tile covers a region 0.1×0.1 in $\Delta\eta$ and $\Delta\phi$ and preserves the semi-projective tower structure of the DØ detector. The modules are placed between the central and endcap cryostats and are mounted on the endcap cryostat walls in an annular structure covering 2π in azimuth (ϕ) and a region $0.8 < |\eta| < 1.4$. For triggered events, the pulse height information from the ICD is digitized and recorded in the calorimeter data stream and is treated as another layer of calorimetry.

The massless gap modules are constructed and read out the same as the calorimeter modules, except the uranium plates are replaced with thin ground planes which are essentially massless. The CC massless gaps have copper clad G10 instead of uranium plates and the EC massless gaps have copper clad G10 in the center and steel on the outside. Each massless gap has 2 signal boards, 3 ground planes and 4 liquid argon gaps and is approximately 1.5 cm thick. The CC massless gaps are positioned inside the central cryostat after the stainless steel end plates of the modules and cover a region $0.7 < |\eta| < 1.2$. The EC massless gaps are positioned after the

endcap cryostat walls and cover a region $0.7 < |\eta| < 1.3$.

3. Test Beam Results

3.1. Configuration

A portion of the DØ calorimeter was exposed to single particles of known energy in the Neutrino-West beam line at Fermilab during the fixed target run from July 1991 through January 1992⁴. The DØ test setup consisted of central and endcap calorimeter modules and the ICD and massless gaps which were placed inside the same cryostat which was filled with liquid argon. The cryostat walls, dead materials and regions with no argon in the DØ experiment were simulated in this setup. Coverage of the calorimeter modules extended from -1.2 to 1.6 radians in η , and there was full η coverage of the ICD and massless gaps. The azimuthal coverage was 1/8 of the full calorimeter. A transporter allowed rotation of the cryostat so that the incident beam struck the modules at different η values along the semi-projective towers which pointed to the DØ vertex.

3.2. Data Analysis and Results

Data taken using a π^- beam was used to determine the relative enhancement of the energy measurement by the calorimeter when including the ICD and massless gaps. Raw calorimeter data was pedestal subtracted and then corrected by the electronic gain of each channel, which was measured in dedicated pulser runs. The data from ICD modules were first normalized to their MIP signals, obtained by exposing each module to muons, and then corrected by their electronic gains. A multiplicative sampling weight was applied to the data as a function of layer to obtain the energy³.

The first step in the data analysis was to determine the optimal sampling weights for the calorimeter by minimizing the energy resolution. This was done using pions which shower totally in the central calorimeter, and whose momenta were measured independently using tracking chambers. The next step was to determine the sampling weights for the ICD and massless gaps by optimizing the energy resolution in the intermediate η regions. The previously obtained sampling weights for the calorimeter were held fixed and the sampling weights for the ICD and massless gaps were allowed to vary.

The difference in the energy measurements and resolution of the calorimeter with and without the ICD and massless gaps for a 100 GeV π^- beam incident at $\eta = 1.25$ is shown in Figure 2a. The response of the calorimeter varies with η . Figure 2b shows the measured energy in the calorimeter, with and without the ICD and massless gap contributions, as a function of η in a region where the shower is totally in the central calorimeter and in the intermediate η region. As seen from these figures, the use of the ICD and massless gaps greatly improves the energy measurement and resolution.

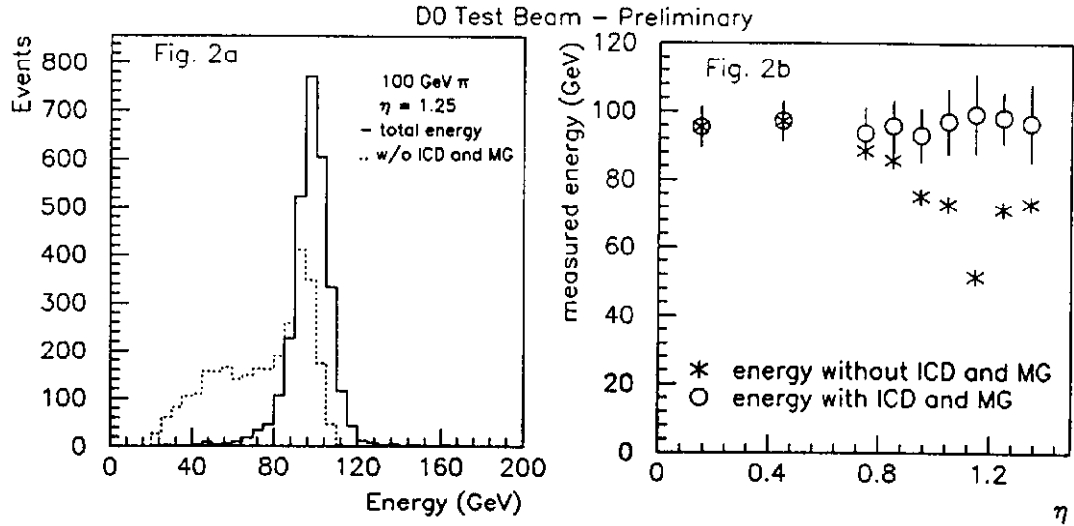


Figure 2: a). energy distribution with and without ICD and massless gap measurements at $\eta = 1.25$ for 100 GeV π data, b). energy measurements as a function of η with and without ICD and massless gap measurements

4. Collider Results

The D0 experiment has been collecting data from the Fermilab $p\bar{p}$ collider since June 1992. Data from a trigger on single jets with E_T greater than 30 GeV was used to compare jets with and without the ICD and massless gap energy measurements. Two-jet events were selected from a data sample and required to be back-to-back within $\Delta\phi < 0.4$ radians. The $|\eta|$ of jet 1 was required to be less than 0.5 radians and jet 2 was required to have an $|\eta|$ greater than that of jet 1. The asymmetry of the two-jet events was defined as

$$A = \frac{E_{T2} - E_{T1}}{1/2(E_{T1} + E_{T2})}$$

and gives a measure of how well the jets are balanced. Figure 3 shows the asymmetry as a function of the η of jet 2, with and without the ICD and massless gaps. The inclusion of the ICD and massless gaps energy measurements greatly improves the matching of the transverse energy of the two jets, as observed in the intermediate η range.

5. Missing E_T Resolution

Good missing E_T resolution (ϕ_T) is important in the analysis of data to determine the mass of the W and for new particle searches. Sources of \cancel{E}_T in the

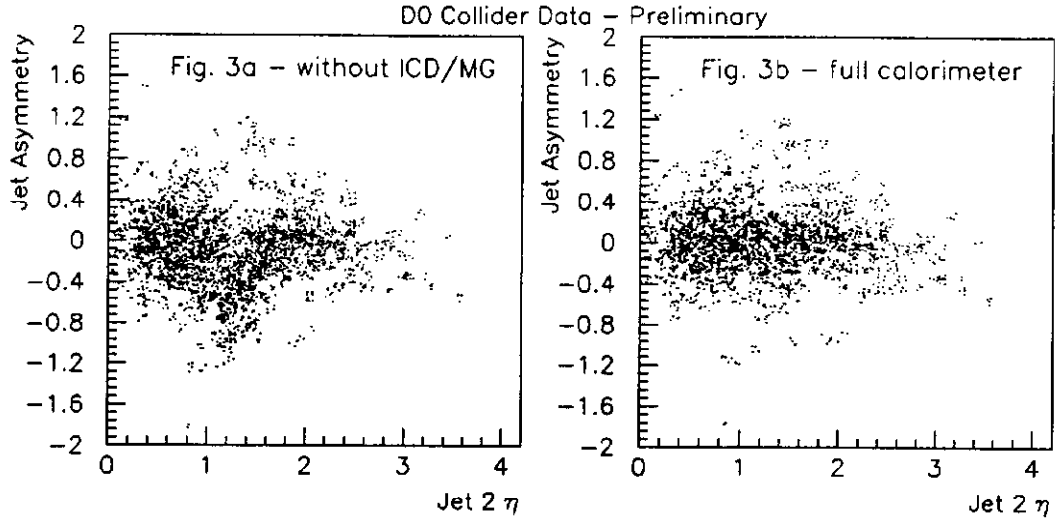


Figure 3: a). jet asymmetry without ICD and MG measurements, b). jet asymmetry with ICD and MG measurements

calorimeter are μ and ν and any other particles that don't interact in the calorimeter. Detector sources include holes for the beam pipe, energy and angular resolution, and noisy or missing readout cells. Minimum bias data allows measure of the \cancel{E}_T due entirely to the detector, because it has negligible contributions from hard-scattering processes which produce particles that don't interact in the calorimeter.

In the analysis presented here⁵, one data run taken from the $p\bar{p}$ collider with a minimum bias trigger was used and no cuts were placed on the data. The \cancel{E}_T is defined as

$$\cancel{E}_x = - \sum_{i=1}^n E_i \sin \theta_i \cos \phi_i,$$

$$\cancel{E}_y = - \sum_{i=1}^n E_i \sin \theta_i \sin \phi_i,$$

$$\cancel{E}_T = \sqrt{\cancel{E}_x^2 + \cancel{E}_y^2},$$

where i runs over the n readout cells of the calorimeter, E_i is the energy deposited in cell i , and θ and ϕ are the polar and azimuthal angles, respectively, of the center of cell i as measured from the vertex of the event. The \cancel{E}_T distribution is shown in Figure 4a. One event in the figure is due to a noisy cell. An algorithm to remove events due to noisy cells in the missing E_T trigger from the data stream is currently in progress.

The \cancel{E}_T distribution is non-Gaussian, however, if we assume the x and y components of the distribution are normally distributed with zero mean and equal

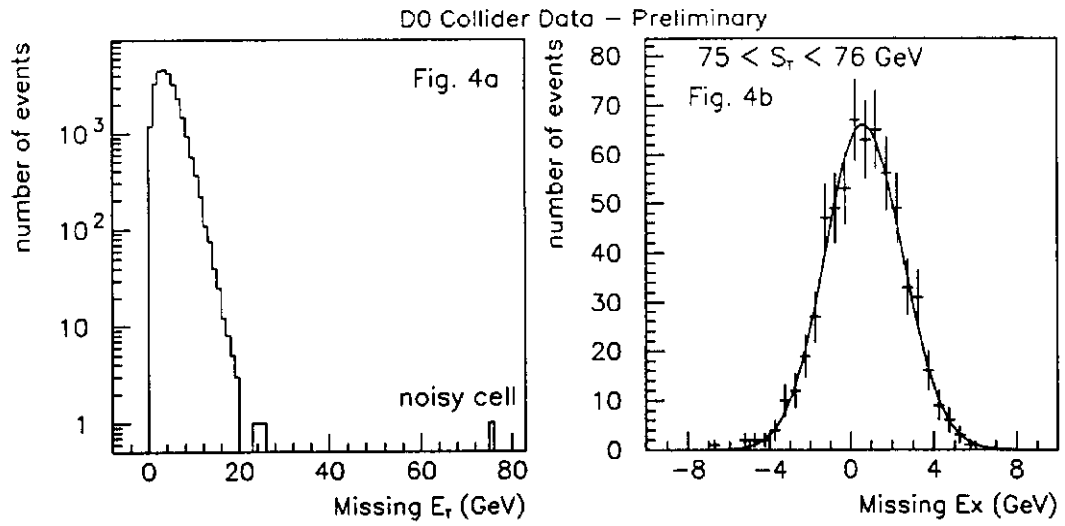


Figure 4: a). \cancel{E}_T distribution b). \cancel{E}_x distribution over range $75 < S_T < 76$ GeV

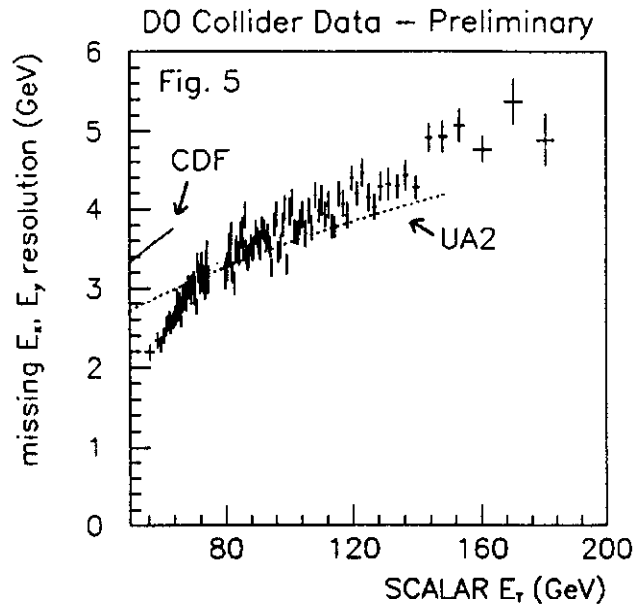


Figure 5: $\cancel{E}_{x,y}$ vs. S_T for $D\bar{D}$ collider data - also shown are the published CDF (solid line) and UA2 (dotted line) results

widths, then the \cancel{E}_T distribution has the form

$$(\cancel{E}_T / \sigma^2) e^{-\cancel{E}_T^2 / 2\sigma^2} \quad (1)$$

where $\sigma \equiv \phi_x \equiv \phi_y \equiv \sqrt{\frac{2}{4-\pi}} \phi_T$. Figure 4b shows the Gaussian \cancel{E}_x distribution over a representative scalar transverse energy (S_T) range from 75 to 76 GeV, where $S_T = \sum_i E_i \sin \theta_i$. The \cancel{E}_T distribution is fit to the form in Eq.(1) in bins of S_T and the resulting $\phi_{x,y}$ is shown in Figure 5 as a function of S_T . Also shown in Figure 5 are the resolutions published by the CDF⁶ and UA2⁷ collaborations over their quoted scalar energy ranges.

6. Conclusions

The DØ calorimeter energy measurement and resolution is greatly improved by the inclusion of the ICD and the massless gaps. The $\cancel{E}_{x,y}$ resolution of the DØ calorimeter varies from ≈ 2.2 to 5.4 GeV over a range of scalar E_T from 60 to 180 GeV for uncorrected minimum bias data.

Acknowledgements

I would like to thank Kaushik De and Marc Paterno for their help in preparing this paper.

References

1. J. Christenson, These Proceedings.
2. S. Abachi et. al., FNAL-PUB-92/162-E, to be published in *Nucl. Instrum. Meth. A*.
H. Aihara et. al., LBL-31378, to be published in *Nucl. Instrum. Meth. A*.
M. Fatyga, These Proceedings.
D. Stewart, These Proceedings.
3. K. De and T. L. Geld, Internal DØ note 1272.
4. K. De, "Tests of the DØ Calorimeter Response in 2 – 150 GeV Beams", to be published in the Proceedings of the XXVI International Conference on High Energy Physics, Dallas, Texas, U.S.A. (1992).
5. M. Paterno, Internal DØ note 1374.
6. F. Abe et. al., *Phys. Rev. Lett.* **65** (1990) 2243.
7. J. Alitti et. al., *Phys. Lett. B* **235** (1990) 363.